THE JOURNAL OF BIOLOGICAL CHEMISTRY VOL. 286, NO. 25, pp. 22122–22130, June 24, 2011

Amyloid-β Annular Protofibrils Evade Fibrillar Fate in Alzheimer Disease Brain*[S]◆

Received for publication, March 1, 2011, and in revised form, April 13, 2011 Published, JBC Papers in Press, April 20, 2011, DOI 10.1074/jbc.M111.236257

Cristian A. Lasagna-Reeves[‡], Charles G. Glabe[§], and Rakez Kayed[‡1]

From the [‡]Department of Neurology, the George P. and Cynthia Woods Mitchell Center for Neurodegenerative Diseases, University of Texas Medical Branch, Galveston, Texas 77555-1045 and the [§]Department of Molecular Biology and Biochemistry, University of California, Irvine, California 92697

Annular protofibrils (APFs) represent a new and distinct class of amyloid structures formed by disease-associated proteins. *In vitro*, these pore-like structures have been implicated in membrane permeabilization and ion homeostasis via pore formation. Still, evidence for their formation and relevance *in vivo* is lacking. Herein, we report that APFs are in a distinct pathway from fibril formation *in vitro* and *in vivo*. In human Alzheimer disease brain samples, amyloid-β APFs were associated with diffuse plaques, but not compact plaques; moreover, we show the formation of intracellular APFs. Our results together with previous studies suggest that the prevention of amyloid-β annular protofibril formation could be a relevant target for the prevention of amyloid-β toxicity in Alzheimer disease.

Many age-related neurodegenerative diseases are characterized by the accumulation of amyloid deposits derived from a variety of misfolded proteins (1). These diseases typically have both sporadic and inherited forms, and in many cases, the mutations associated with the familial forms are in the gene encoding the protein that accumulates or in genes directly related to its production, processing, or accumulation (2). The genetic linkage between the mutant allele and disease is evidence of the causal relationship of amyloid accumulation to pathogenesis. Many of the mutations destabilize the natively folded state, produce more amyloidogenic protein, or increase its propensity to aggregate (3). Although fibrillar amyloid deposits are among the most obvious pathognomonic features of disease, their role in pathogenesis is not clear. The extent of fibrillar amyloid plaque deposition does not correlate well with the pathogenesis of Alzheimer disease (AD),[2] and a significant number of non-demented individuals have amounts of amyloid plaque equivalent to disease patients (4). Pathological changes are observed in transgenic animals prior to the onset of amyloid plaque accumulation (5, 6), and it has been reported that soluble amyloid-β (Aβ) oligomers correlate better with dementia than do insoluble fibrillar deposits (7, 8), suggesting that oligomeric forms of Aβ may represent the primary toxic species. Soluble oligomers have been implicated as the primary toxic species in many degenerative diseases in which the accumulation of large fibrillar deposits may be inert, protective, or pathological by a different mechanism (9, 10). However, their structures, interrelationships with other amyloid aggregates, and exact contribution to disease pathogenesis are not entirely clear (11–13). Aβ and other amyloidogenic proteins form annular protofibrils (APFs) *in vitro*; these pore-like structures have been observed in preparations of both oligomers and fibrils (14, 15). The formation of pores by Aβ and α-synuclein was accelerated by mutations associated with familial Alzheimer and Parkinson diseases, respectively, suggesting that their formation is related to pathogenic activity (16).

The amyloid pore hypothesis (17) suggests that amyloid oligomers/protofibrils cause cell death by disrupting regulated membrane permeability, similar in mechanism to bacterial pore-forming toxins (18–20), which leads to disruption of cellular ion and protein homeostasis. Membrane permeabilization is a common pathogenic activity of amyloid oligomers (21), which are a precursor to APF formation. The formation of APFs is an attractive explanation for the membrane permeabilization of oligomers because of a shared assembly state and the morphological resemblance between APFs and pores.

Despite the overwhelming quantity of data from biochemical, biophysical, and cell culture experiments supporting amyloid pore formation (17), evidence for Aβ pore formation in AD brains is sparse. The purpose of this study was to determine the relationship of Aβ APFs with other Aβ amyloid species and to clarify the presence of APFs in the brains of AD patients. Herein, we demonstrated that APFs are on a distinct pathway from amyloid fibril formation evading fibrillar fate and that these pore-like structures are present in AD human brain tissue.

EXPERIMENTAL PROCEDURES

Preparation and Characterization of Amyloid-β Oligomers, Fibrils, and Annular Protofibrils—Aβ was synthesized by Fmoc *N*-(9-fluorenyl)methoxycarbonyl chemistry using a continuous flow semiautomatic instrument as described previously (22). Aβ oligomers and fibrils were prepared as described previously (23). Briefly, fibrils were prepared in water (pH 3.8–4.2) containing 0.02% sodium azide. The samples were stirred with a Teflon-coated micro stir bar at 500 rpm at room temperature

* This work was supported by grants from the Alzheimer's Association, the Mitchell Center for Neurodegenerative Diseases, and the Cullen Trust.
◆ This article was selected as a Paper of the Week.
[S] The on-line version of this article (available at http://www.jbc.org) contains supplemental Figs. 1 and 2.
[1] To whom correspondence should be addressed: Dept. of Neurology, University of Texas Medical Branch, 301 University Blvd., Medical Research Bldg., Rm. 10.138C, Galveston, TX 77555. Tel.: 409-772-0138; Fax: 409-747-0015; E-mail: rakayed@utmb.edu.
[2] The abbreviations used are: AD, Alzheimer disease; Aβ, amyloid-β; APF, annular protofibril; Bis-Tris, 2-(bis(2-hydroxyethyl)amino)-2-(hydroxymethyl)propane-1,3-diol.

for 6–9 days. Fibril formation was monitored by thioflavin T fluorescence (data not shown). Once fibril formation was complete, the solutions were centrifuged at 14,000 × *g* for 20 min, and the fibril pellet was washed three times with doubly distilled water and then resuspended in the desired buffer. Soluble oligomers were prepared by dissolving 1.0 mg of Aβ in 400 μl of hexafluoroisopropanol for 10–20 min at room temperature. Then, 100 μl of the resulting seedless Aβ solution was added to 900 μl of double distilled H_2O in a siliconized Eppendorf tube. After a 10–20-min incubation at room temperature, the samples were centrifuged for 15 min at 14,000 × *g*, and the supernatant fraction (pH 2.8–3.5) was transferred to a new siliconized tube and subjected to a gentle stream of N2 for 5–10 min to evaporate the hexafluoroisopropanol. The samples were then stirred at 500 rpm using a Teflon-coated micro stir bar for 24–48 h at 22 °C (23–25). A homogeneous population of annular (pore-like) protofibrils was achieved by using oligomers as the starting material. Five percent (v/v) of hexane was added to a solution of oligomers, and the sample was mixed with a vortex mixer for 1 min every 5 min for a total of 50 min. Afterward, the samples were dialyzed in water, using a molecular mass cut-off membrane of 10 kDa.

The morphology of oligomers, fibrils, and annular protofibril preparations was assessed by electron microscopy. Two microliters of each sample was adsorbed onto 200-mesh carbon and Formvar-coated grids, air-dried, and washed for 1 min in distilled water. The samples were negatively stained with 2% uranyl acetate (Ted Pella Inc., Redding, CA) for 2 min and viewed with a Zeiss 10CR microscope (80 kV).

Liposome Preparation—Ten milligrams of phosphatidylcholines (Sigma) was dissolved in 500 μl of chloroform (20 mg/ml). The chloroform was evaporated under a stream of nitrogen in the hood, and then the film was hydrated with 500 μl of buffer (10 mM HEPES, 100 mM NaCl, pH 7.4) and finally vortexed intensely for 3–5 min. Aβ oligomers were prepared at 66 μM in H_2O and incubated at room temperature with liposomes in phosphate-buffered saline (PBS; 1/10 (v/v) liposome/Aβ oligomers) for 2 h.

Immunolabeling of Amyloid-β Annular Protofibrils in Vitro—Liposomes incubated with Aβ oligomers for 2 h, liposomes just mixed with Aβ oligomers (without incubation), liposomes and without Aβ oligomers stirred for 2 h were centrifuged at 35,000 × *g* for 90 min at 4 °C. Pellets were rinsed and resuspended in 20 mM HEPES, and portions of each sample were deposited on glass coverslips for 20 min followed by rinses with PBS and fixation for 10 min with 4% paraformaldehyde. Each sample was washed with PBS and with PBS containing 3% bovine serum albumin and 1% goat serum. The samples were incubated with αAPF antibody (1:700), A-11 antibody (1:1000), or OC antibody (1:2000) overnight at 4 °C. After washing with PBS, the sample was incubated with Alexa Fluor 568-conjugated goat anti-rabbit IgG (1:700) for 1 h at room temperature. For the double immunofluorescence with 4G8, samples were first incubated with αAPF and the secondary Alexa Fluor 568 goat anti-rabbit and then with 4G8 (1:800) overnight at 4 °C. The next day, samples were washed with PBS and incubated with Alexa Fluor 488 goat anti-mouse antibody (1:700). In the case of the double immunofluorescence between A-11 and αAPF, samples were incubated first with A-11 and with Alexa Fluor 568 goat anti-rabbit antibody. Then, samples were refixed with 16% paraformaldehyde for 3 h. After this, samples were washed with PBS and incubated overnight with αAPF and the next day with Alexa Fluor 488 goat anti-rabbit antibody for 1 h. Fluorescence images were captured using an epifluorescence microscope (Nikon Eclipse 800) equipped with a CoolSnap-FX monochrome CCD camera (Photometrics, Tucson, AZ).

Brain Samples—Frozen AD human brain tissues and age-matched controls were obtained from the Alzheimer's Disease Research Center Tissue Repository at the University of California at Irvine Institute for Brain Aging and Dementia. The following information was available for each case: Braak and Braak stage, postmortem index, gender, age at death, and Mini-Mental State Examination score (39, 40).

Annular Protofibril Immunostaining Using the 3,3′-Diaminobenzidine Method—Brain tissue paraffin sections were hydrated using xylene, 100% ethanol, 95% ethanol, 80% ethanol, and distilled water. The hydrated sections in target solution (Dako, Carpinteria, CA) were heated twice for 5 min each using a microwave oven (750 watts). Tissues were next washed in 1× PBS, three times for 5 min each, and blocked for 10 min with 3% H_2O_2 in PBS. Tissues were then washed in 1× PBS, three times for 5 min each, and blocked for 60 min with 5% horse serum in PBS. The tissues were incubated with the αAPF antibody (1:350) overnight. The sections were washed three times with 1× PBS for 10 min for each wash. The sections were next incubated with the secondary antibody, biotinylated anti-rabbit (Pierce Biotechnology), for 60 min. The sections were washed three times, 5 min each time, with 1× PBS. The sections were then incubated 30 min using an ABC kit and washed with 1× PBS three times for 5 min each. Finally, the sections were incubated with 3,3′-diaminobenzidine for 5 min.

Immunoprecipitation of Annular Protofibrils from Human Brain Tissue—Brain frontal cortex tissues from three age-matched non-demented controls and three AD brains were homogenized in PBS containing a mixture of protease inhibitors (diluted 1:100, Sigma P-2714) and ultracentrifuged at 78,400 × *g* for 1 h at 4 °C. The supernatant was collected, aliquoted, and stored at −80 °C. Total protein concentration was determined by the bicinchoninic acid (BCA) protein assay, and the concentration of the samples was normalized.

For immunoprecipitation experiments, tosyl-activated magnetic Dynabeads (Dynal Biotech, Lafayette Hill, PA) were coated with 11.25 μg of αAPF antibody (2.6 mg/ml) diluted in 0.1 M borate, pH 9.5, overnight at 37 °C. Beads were washed (0.2 M Tris, 0.1% bovine serum albumin, pH 8.5) and then incubated with either AD or normal patient brain homogenates with rotation at room temperature for 1 h. Beads were then washed three times with PBS and eluted using 0.1 M glycine, pH 2.8. The pH of each eluted fraction was adjusted using 1 M Tris, pH 8.0.

The morphology of immunoprecipitated structures was assessed by electron microscopy. Two to four microliters of the eluted samples was adsorbed onto 200-mesh carbon and Formvar-coated nickel grids, air-dried, and washed for 1 min in distilled water. The samples were negatively stained with 3 μl of 2% uranyl acetate for 2 min and viewed with a Zeiss 10CR microscope (80 kV).

Western Blot Analysis of PBS-soluble Fraction with α-Annular Protofibril Antibody—Tissue samples were diced and homogenized in 5% w/v ice-cold PBS with protease inhibitor mixture and 0.02% NaN_3. Homogenates were centrifuged for 10 min at 3000 × *g*. The total protein concentration of all samples was determined by BCA assay and normalized with 1× PBS. Proteins in the supernatant were mixed with 4× sample buffer, loaded (without boiling), separated by SDS-PAGE using 4–12% Bis-Tris gels (Invitrogen), and transferred onto nitrocellulose. After blocking with nonfat dried milk, membranes were probed with αAPF antibody (1:700). Antibody immunoreactivity was detected with horseradish peroxidase-conjugated anti-rabbit IgG (1:3000, The Jackson Laboratory, Bar Harbor, ME) followed by electrochemiluminescence.

Double Immunofluorescence with α-Annular Protofibril and 4G8 Antibodies—The sections in paraffin were hydrated using xylene, 100% ethanol, 95% ethanol, 80% ethanol, and distilled water. Then, the sections were heated by microwave (750 watts) in target solution (Dako) twice for 4 min each. The tissues were washed in 1× PBS, three times for 5 min each, and blocked for 45 min with 5% horse serum in PBS. The tissues were incubated with αAPF antibody (1:350) overnight. After this, the sections were washed three times with 1× PBS for 10 min for each wash. The sections were incubated with the secondary antibody anti-rabbit Alexa Fluor 568 (1:700; Molecular Probes, Eugene, OR) for 60 min. Then, the sections were washed three times with 1× PBS, for 5 min each, and blocked again with 5% horse serum in PBS for 30 min. The sections were incubated with the primary, Aβ-specific antibody 4G8 (1:800) overnight. The sections were washed with 1× PBS, three times for 10 min for each wash. The sections were incubated with the secondary antibody anti-mouse Alexa Fluor 488 (Molecular Probes) for 60 min. Then, the sections were washed with 1× PBS, three times for 5 min each. Finally, the sections were incubated with TO-PRO-3 (1:2000; Molecular Probes) for 5 min to stain the nuclei. The double staining with A-11 and αAPF was performed as described for αAPF and 4G8 antibodies, with the following modifications. After the overnight incubation with αAPF and the incubation for 1 h with the secondary antibody anti-rabbit Alexa Fluor 488 (Molecular Probes), sections were washed three times in 1× PBS and incubated for 2 h with 16% paraformaldehyde at room temperature. Then, the sections were washed three times with 1× PBS, for 5 min each, and blocked again with 5% horse serum in PBS for 30 min. The sections were incubated with the primary, oligomer antibody A-11 (1:1000) overnight. The sections were washed with 1× PBS, three times for 10 min for each wash. The sections were incubated with the secondary antibody anti-rabbit Alexa Fluor 488 (Molecular Probes) for 60 min. Then, the sections were washed with 1× PBS, three times for 5 min each. Finally, the sections were incubated with TO-PRO-3 (1:2000; Molecular Probes) for 5 min to stain the nuclei. Intensity correlation analysis was performed as described in detail by Li *et al.* (26) and using the ImageJ software (National Institutes of Health, Bethesda, MD).

Antibody Blocking Experiment—The antibody αAPF was preincubated for 40 min with its antigen APFs. After the incubation period, this antibody was used to perform light field immunohistochemistry and double immunofluorescence experiments with 4G8 in AD brain sections that were confirmed to be positive for APFs.

RESULTS

Annular Protofibrils Evade Fibrillar Fate—Previously, we showed that spherical Aβ oligomers can assemble into Aβ pores and that their assembly follows a pathway parallel to fibril formation (18). It has also been demonstrated that amyloid pores from different amyloidogenic proteins resemble the pores formed by bacterial toxins (20). They are similar in morphology and conformation, evident by their immunoreactivity with αAPF antibody generated against homogeneous populations of Aβ annular protofibrils (18).

To investigate the complete independence between Aβ APF and Aβ fibril pathways, we prepared and characterized a homogeneous population of APFs (Fig. 1, *A* and *C*) and Aβ fibrils (Fig. 1, *B* and *D*). As we previously showed (18), there was no formation of fibrils in the APF preparation. When APFs were incubated with Aβ fibrils from 48 h (Fig. 1*E*) up to 30 days (Fig. 1*F*), APFs did not form fibrils, contradictory to what happened when Aβ oligomers were mixed with fibrils (supplemental Fig. 1). In the case of oligomers, they changed their conformation and promoted fibril elongation (supplemental Fig. 1). As we already showed, liposomes can catalyze the conversion of oligomers to APFs under more physiological conditions than treatment with 5% hexane (18). When liposomes were reconstituted with Aβ oligomers and incubated for 2 h, they were immunolabeled with A-11 (anti-oligomer antibody) (Fig. 1*G*) and αAPF (anti-APF antibody) (Fig. 1*H*) but not with OC (anti-fibril antibody) (Fig. 1*I*). When liposomes were immediately mixed with Aβ oligomers without incubation, they were immunolabeled only with A-11 (Fig. 1*J*) but not with αAPF (Fig. 1*K*) or OC (Fig. 1*L*). On the other hand, in samples prepared from oligomers stirred for 2 h without the presence of liposomes, immunolabeling was observed for A-11 (Fig. 1*M*) and OC (Fig. 1*O*) but not for αAPF (Fig. 1*N*). Immunofluorescence was not observed in liposomes reconstituted without Aβ oligomers (Fig. 1, *P–R*). Overall, these results confirm and demonstrate that Aβ APFs are on a distinct pathway from amyloid fibril formation and evade fibrillar fate *in vitro*.

Amyloid-β Annular Protofibrils Are Present in Alzheimer Disease Brain Tissue and Are on a Distinct Pathway from Compact Plaque Formation—In the AD transgenic mouse model (APP23), αAPF antibody staining revealed that APFs are ultrastructurally localized to plasma membranes and vesicles inside of cell processes (27). To investigate the presence of pore-like structures in human AD brains, we used αAPF antibody, which enabled us to distinguish them from other amyloid aggregates. Immunohistochemistry using αAPF antibody in the 3,3′-diaminobenzidine method revealed strong immunostaining associated with diffuse plaques and intracellular punctate deposits located mainly around the nucleus (Fig. 2, *A–E*). αAPF immunoreactivity was absent in sections collected from age-matched control brains (Fig. 2*F*). Pore-like structures from human AD frontal cortex tissues were isolated by immunoprecipitation using αAPF antibody. Subsequent examination by electron microscopy (Fig. 2, *G–J*), showed these structures to be morphologically similar to amyloid pores prepared *in vitro*.

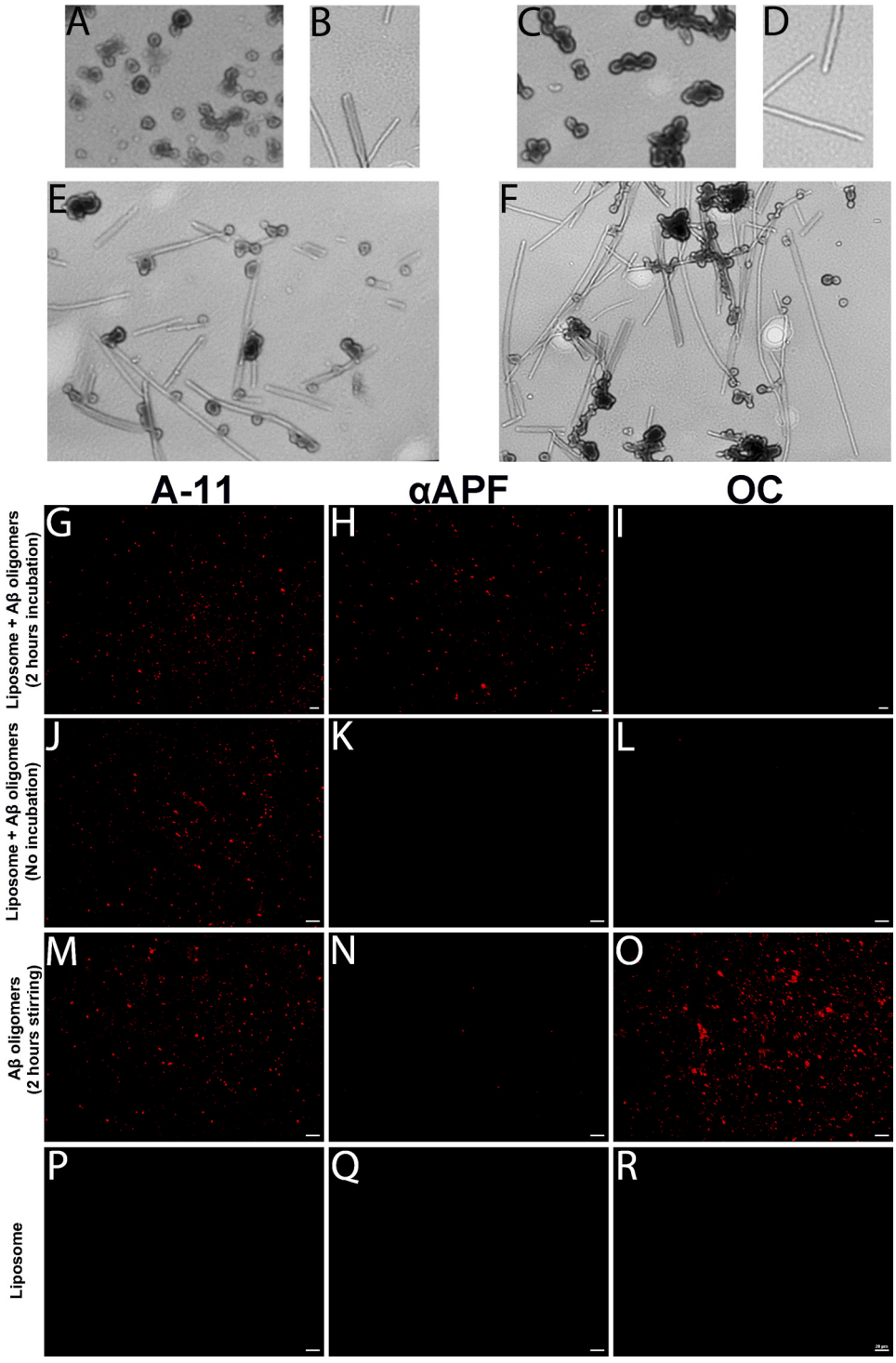

FIGURE 1. **Annular protofibrils evade fibrillar fate.** *A–F*, pure Aβ APFs (*A* and *C*) were incubated with pure Aβ fibrils (*B* and *D*) for 48 h (*E*) up to 30 days (*F*). APFs do not convert to fibrils, as is common for oligomers, showing that APFs evade fibrillar fate. *G–I*, liposomes reconstituted with Aβ oligomers and incubated for 2 h exhibit punctate immunofluorescence for oligomers (*A-11 column*) and αAPFs but not for fibrils (*OC column*), suggesting that oligomers convert to APFs in the presence of membranes but not to fibrils. *J–L*, liposomes reconstituted with Aβ oligomers without incubation only exhibit punctate immunofluorescence for oligomers. *M–O*, when oligomers were stirred for 2 h without liposomes, oligomers and fibrils were detected but not APFs. *P–R*, as a negative control, liposomes alone were stained with A-11 and αAPF.

Surprisingly, they were more homogeneous than those imaged from *in vitro* preparations (18). The brain-derived pore size was roughly 11–14 nm in outer diameter and 2.5–4 nm in inner diameter. Additionally, immunoprecipitation from non-AD control tissues did not yield any amyloid pores that were visible by electron microscopy (Fig. 2*K*). Western blot analysis of human brain PBS-soluble fraction confirmed the presence of APFs in AD cases (Fig. 2*L*). This demonstrates the formation of amyloid pores in AD brains and suggests that amyloid pores may play a significant role in cognitive dysfunction present with AD.

To confirm that the APFs detected in AD samples were indeed Aβ annular protofibrils, we performed double immuno-

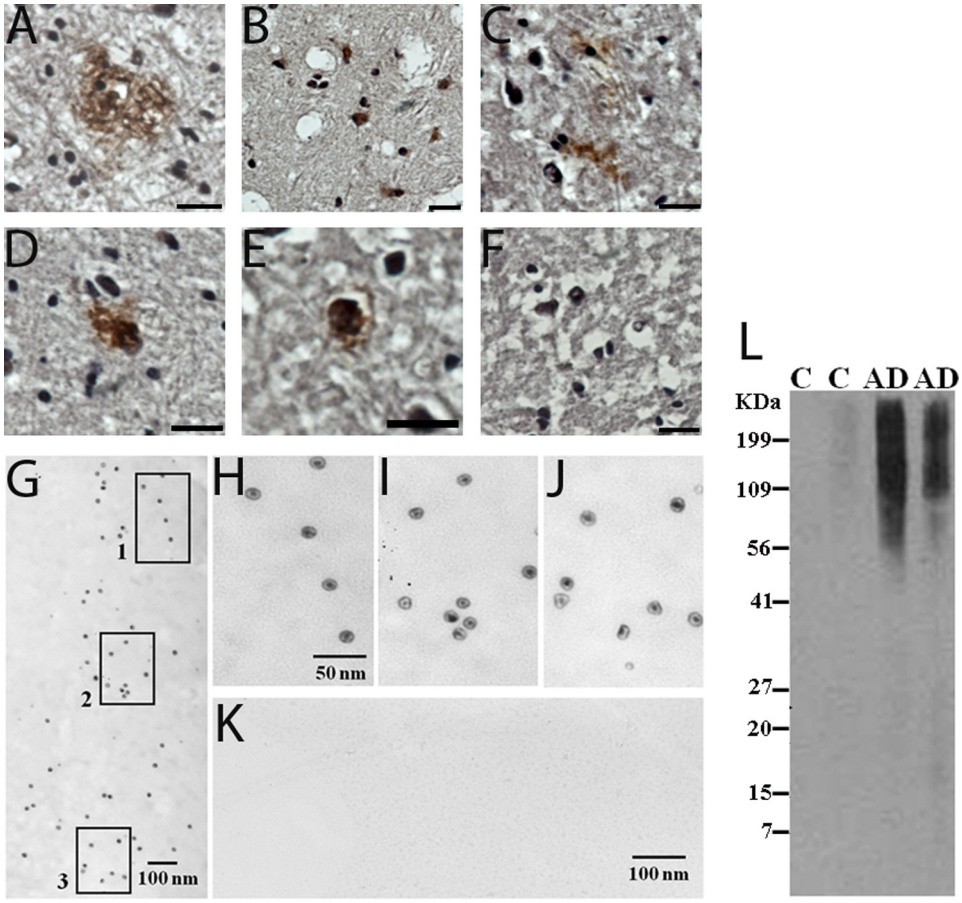

FIGURE 2. **Detection of amyloid pores in tissues from Alzheimer disease brains.** *A–E*, amyloid pores were detected in AD brain frontal cortex sections by light field microscopy after immunostaining using the 3,3′-diaminobenzidine method. The pore-like structures were present in diffuse plaques and as punctate, diffuse deposits mainly located around the nucleus, which was stained with hematoxylin. *F*, no amyloid pores were detected in tissues from age-matched control brains. (*Scale bars* represent 20 μm.) *G–J*, amyloid pores were isolated by immunoprecipitation using αAPF antibody and visualized by electron microscopy. *Images H*, *I*, and *J* are magnifications of *squares 1*, *2*, and *3*, respectively. *K*, no amyloid pores were pulled down by immunoprecipitation from age-matched controls. Micrographs represent immunoprecipitation from three AD cases and three control cases. *L*, Western blot analysis with αAPF shows that amyloid pores with molecular mass >90 kDa were present only in AD cases (*AD lane*). The control cases (*C lane*) used in this study did not present Aβ amyloid plaques.

fluorescence staining using αAPF antibody and the Aβ-specific antibody 4G8 (Fig. 3). No Aβ pore-like structures were found within the Aβ compact plaques (Fig. 3, *A–F*). This is not surprising because compact plaques are known to contain mainly mature Aβ fibrils. Strong colocalization between αAPF and 4G8 was found intracellularly (Fig. 3, *A–I*) and in extracellular Aβ diffuse plaques (Fig. 3, *J–L*). Whenever the αAPF antibody was preincubated with the antigen APF before performing the immunostaining, no immunolabeling was observed in the AD cases where Aβ APFs were detected, demonstrating the specificity of αAPF for annular protofibrils in human AD sections (supplemental Fig. 2). These results suggest that Aβ APFs follow a distinct pathway from Aβ fibrils *in vivo*.

Oligomers Are a Precursor to Annular Protofibrils in Vivo—We recently demonstrated that the incubation of Aβ oligomers with lipid vesicles results in a rapid loss of the spherical oligomer-specific epitope and the coordinate appearances of an APF-specific epitope, suggesting that the interaction of spherical oligomers with membranes catalyzes their conformational conversion into APF pores (18). To visualize this conversion process, liposomes were reconstituted with Aβ oligomers and incubated for 2 h, and then liposomes were immunolabeled with A-11 (Fig. 4A) and αAPF (Fig. 4*B*). Colocalization of both signals (Fig. 4*C*) after the 2-h incubation demonstrates that the interaction of the oligomers with the liposome induces the conversion to APFs. When liposomes were mixed with Aβ oligomers and immediately visualized without incubation, no APFs were detected (Fig. 4, *D–F*), reaffirming that oligomers must interact with lipidic membranes to induce the conversion to APFs *in vitro*. To investigate this premise *in vivo*, we performed double immunofluorescence in AD brain sections using an anti-oligomer-specific antibody (A-11) (25) (Fig. 4, *M–O*). The colocalization of the signals demonstrated the interactions between these two conformational structures and suggests that spherical oligomers represent the building blocks for pore-like amyloid formation in AD brains.

DISCUSSION

As we previously reported, Aβ oligomers are not only the intermediates of Aβ fibril aggregation but also the precursors of APF formation (27). The findings of the present study suggest that *in vitro* and *in vivo* APFs are on a completely independent pathway from Aβ fibril formation (Fig. 5). It is not clear which is

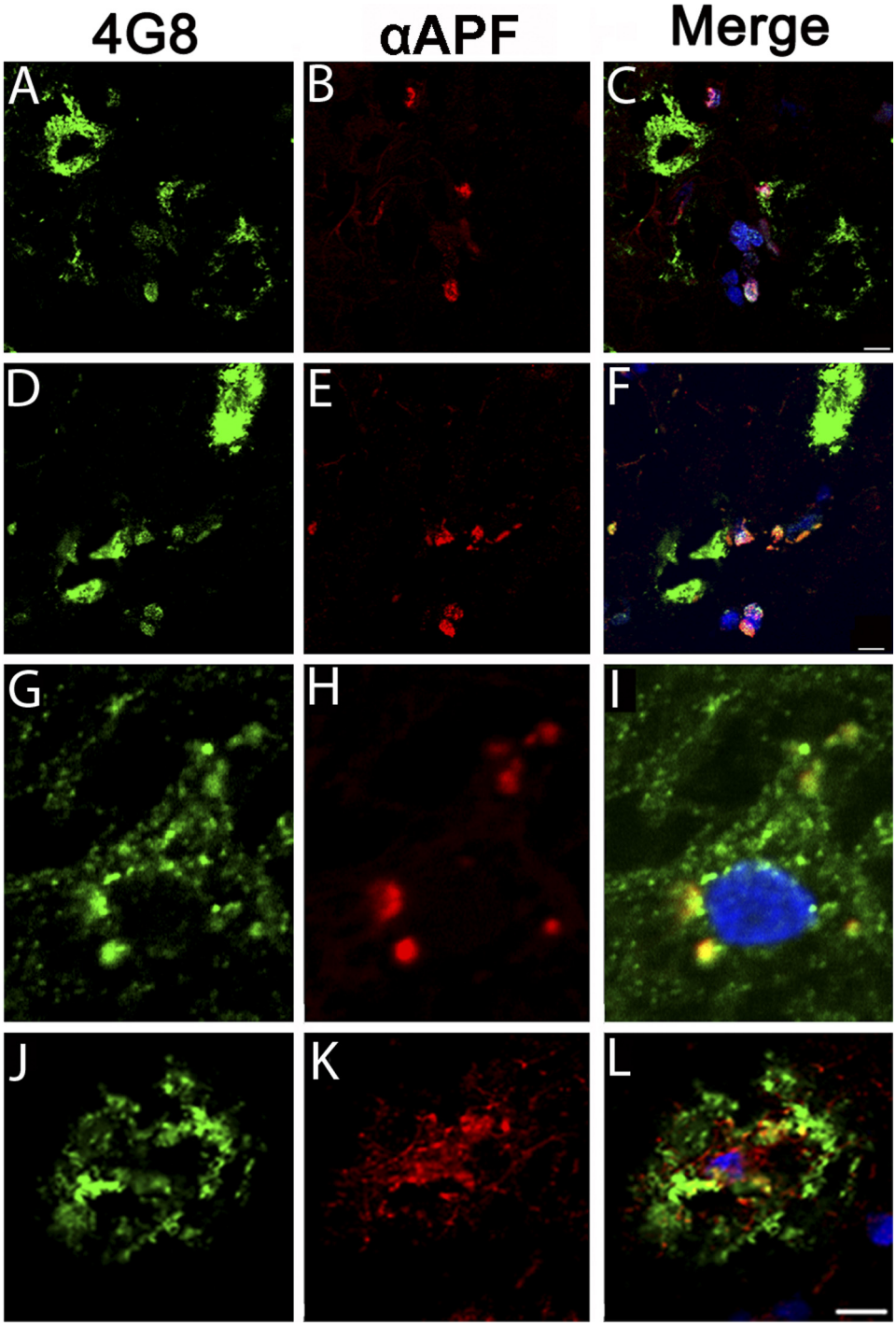

FIGURE 3. **Amyloid-β pores in Alzheimer disease brains were detected intracellularly and in extracellular diffuse plaques but not in compact plaques.** *A–F*, double staining with 4G8 for Aβ (*green fluorescence*) and αAPF (*red fluorescence*) demonstrates that APFs are not associated with compact plaques and are present intracellularly. *G–I*, higher magnification confirmed that Aβ pores are intracellular with a punctate staining pattern characteristic of membrane vesicles. *J–L*, using the same immunostaining method, Aβ pores were also detected in diffuse plaques. (*Scale bars* represent 10 μm). Nuclei were stained with TO-PRO-3.

the determinant of the pathway for Aβ oligomers to form, whether APFs break down and form fibrils or vice versa (Fig. 5). Yamamoto *et al.* (29) demonstrated that cell surface GM1-ganglioside of cultured neurons induces thioflavin S-positive Aβ amyloid, suggesting that GM1-ganglioside may provide the platform for early stages of Aβ fibril aggregation. The mechanism of membrane-catalyzed conformational conversion of Aβ oligomers into Aβ pores is not yet well understood. It is possible that following an initial electrostatic interaction with the membrane, individual spherical oligomers are drawn into the core of the lipid bilayer and consequently undergo a conformational transition to expose their hydrophobic segments and assemble into pore-like structures (12, 30–33). A similar membrane-catalyzed assembly has been proposed for the pore-forming toxins, in which the stepwise binding of toxin to the membrane, membrane-catalyzed conformational change, and toxin oligomeri-

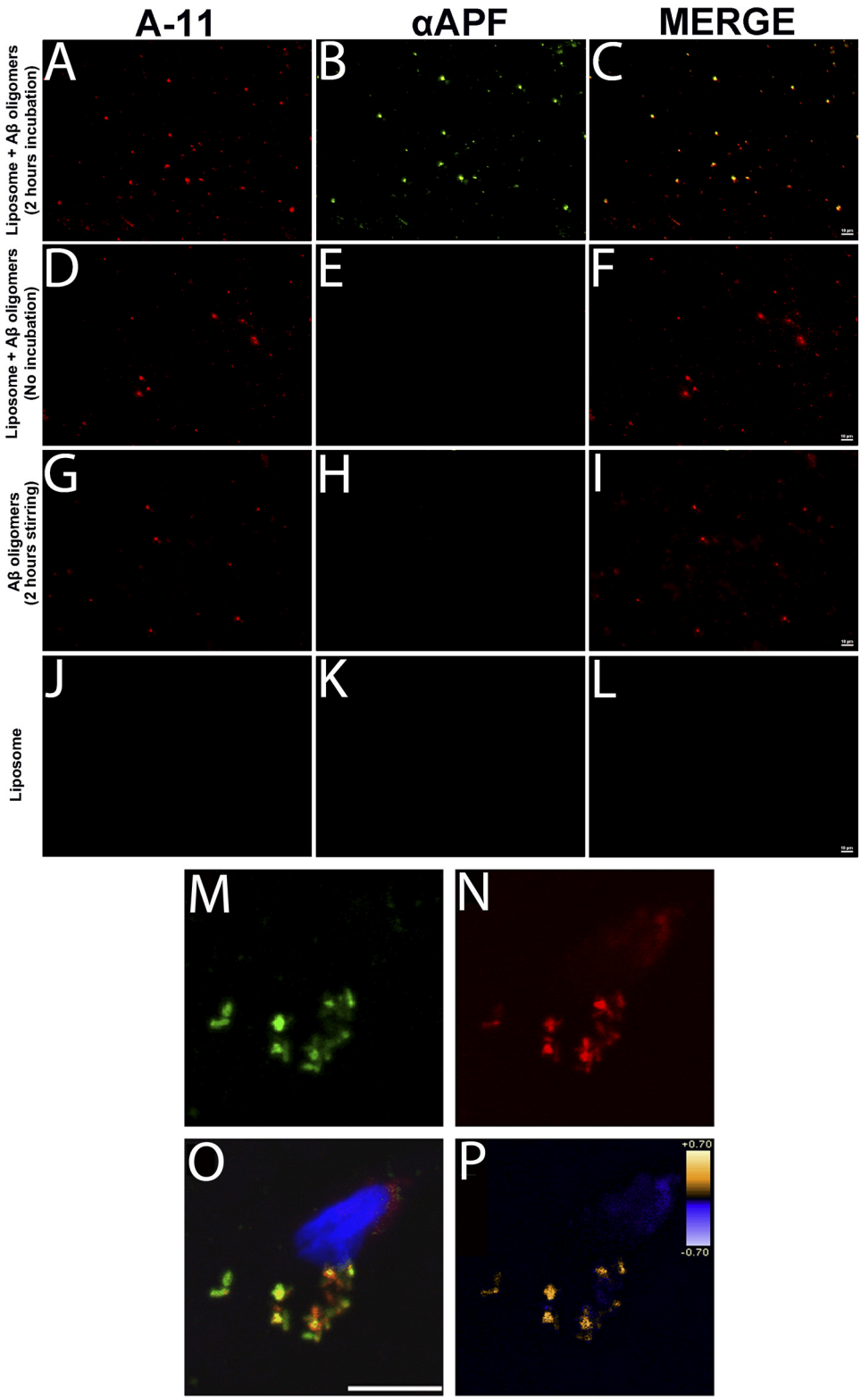

FIGURE 4. **Connection between oligomers and pores in Alzheimer disease brains.** *A–C*, liposomes reconstituted with Aβ oligomers and incubated for 2 h exhibit colocalization between punctate immunofluorescence for oligomers (*A-11 column*, *red*) and APFs (α*APF column*, *green*), suggesting that oligomers convert to APFs. *D–F*, liposomes reconstituted with Aβ oligomers without incubation exhibit only punctate immunofluorescences for oligomers (*A-11 column*, *red*). *G–I*, the same happens with oligomers stirred for 2 h without liposomes; only oligomers were detected. *J–L*, as a negative control, liposomes alone were stained with A-11 and αAPF. *M–O*, double staining in AD brain sections with anti-oligomer specific antibody A-11 (*green fluorescence*) and αAPF antibody (*red fluorescence*) demonstrates the interactions between oligomers and pores *in vivo*. (*Scale bar* represents 10 μm.) *P*, the colocalization of oligomers with pores was confirmed by intensity correlation analysis of the signals. Nuclei were stained with TOP-RO-3.

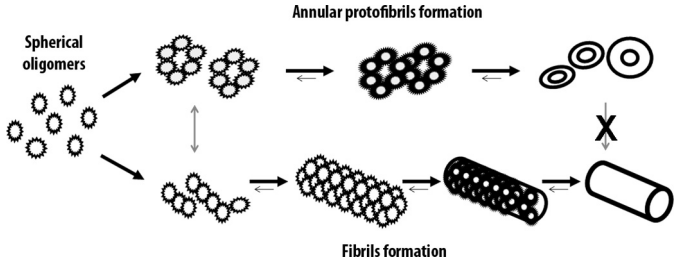

FIGURE 5. **Annular protofibrils are on a distinct pathway from amyloid fibril formation.** A schematic diagram of how APFs and amyloid fibrils originate from spherical oligomers, to follow two independent amyloidogenic pathways, is shown.

zation lead to the formation of membrane-embedded pores (19).

We also acknowledge the possibility that the centrifugation process itself may affect the size and intermolecular interactions of the oligomers and liposomes in our *in vitro* model. To minimize this risk, we have taken great care to standardize these procedures in our laboratory to avoid any conformational change of the protein. In this effort, detergents and denaturing agents are not used in our procedures to ensure that the conformation is unaffected. When liposomes were mixed with oligomers and immediately centrifuged, it was not possible to detect the formation of APFs *in vitro* using immunofluorescence techniques, thereby demonstrating that the centrifugation process does not affect or induce the formation of APFs in liposomes (as shown in Fig. 1, *J–L*).

Electron microscopic analysis of pores isolated from human brains with multiple system atrophy inclusions revealed that they are indeed composed of individual spherical oligomers and vary in shape and size, lending support to the notion of nonspecific pore formation and membrane leakage (34). Nevertheless, other laboratories reported the ability of Aβ to form calcium channels in lipid bilayers and neuronal cells (35, 36). Recently, Jang *et al.* (37) reported the ability of Aβ peptide fragments to form oligomers that assembled into pores with single-channel conductance that allow calcium uptake. Our results do not rule out the possibility of channel activity by the small pores. Recently, Kokubo *et al.* (27) by immunoelectron microscopy using αAPF antibody showed that αAPF immunoreactions tended to be found on plasma membranes and vesicles inside of cell processes in transgenic mice expressing a mutant form of amyloid precursor protein (38).

Collectively, our results suggest that the presence of Aβ pores in AD brains and, *in vitro*, the formation of these structures are on a distinct pathway from Aβ fibrils and could play a critical role in AD pathogenesis. The formation of nonspecific Aβ pores or channels in AD brain cells could eventually lead to cell death. Positive immunolabeling with αAPF was present intracellularly, which is in agreement with previous data in transgenic mice (27) and in diffuse plaques. This last point makes sense if we take into consideration a study from Yamaguchi *et al.* (38), which showed that membrane-bound Aβ was the initial deposition of Aβ in diffuse plaques. Biochemical analysis revealed that Aβ APFs are homogeneous in shape and size *in vivo* and are detected at a high molecular weight in SDS gels. This agrees with the model published by Shafrir *et al.* (28), where it was suggested that APFs are formed by 36 Aβ peptides (~155 kDa). Specifically, the authors suggest that APFs are formed by six Aβ hexamers and that these hexamers may slowly merge to form a smooth APF.

Moreover, our novel findings that link Aβ oligomers with Aβ APFs provide a better understanding of amyloid oligomer-mediated neurodegeneration *in vivo* and underscore the complexity of Aβ structures in AD brains. Understanding the fundamentals of Aβ pore formation and properties *in vivo* is critical for establishing potential links between Aβ aggregation and the mechanisms of cellular toxicity that occur with the progression of AD. Still, further research should be conducted to examine the controversy over the nature of these Aβ pores and to determine whether they represent single channels or nonspecific pores.

In conclusion, the results presented here suggest that *in vivo*, Aβ spherical oligomers assemble into pore-like structures, which are in a distinct pathway from amyloid fibril formation; according to previous data (18), the pore-like structures can compromise the integrity of cellular membranes, thereby causing further damage. However, additional comprehensive studies are required to elucidate the molecular mechanisms behind the cause of amyloid pore/channel formation *in vivo* and to explore a possible therapeutic option.

Acknowledgments—We are grateful to Prof. Carl Cotman and the UCI-ADRC brain bank for providing brain samples, Dr. Erene Mina for assistance with immunoprecipitation experiments, and Prof. George Jackson and Dr. Bridget Hawkins for helpful suggestions.

REFERENCES

1. Dobson, C. M. (2006) *Protein Pept. Lett.* **13,** 219–227
2. Hardy, J. (2005) *Biochem. Soc. Trans.* **33,** 578–581
3. Chiti, F., Stefani, M., Taddei, N., Ramponi, G., and Dobson, C. M. (2003) *Nature* **424,** 805–808
4. Terry, R. D. (1996) *J. Neuropathol. Exp. Neurol.* **55,** 1023–1025
5. Westerman, M. A., Cooper-Blacketer, D., Mariash, A., Kotilinek, L., Kawarabayashi, T., Younkin, L. H., Carlson, G. A., Younkin, S. G., and Ashe, K. H. (2002) *J. Neurosci.* **22,** 1858–1867
6. Billings, L. M., Oddo, S., Green, K. N., McGaugh, J. L., and LaFerla, F. M. (2005) *Neuron* **45,** 675–688
7. McLean, C. A., Cherny, R. A., Fraser, F. W., Fuller, S. J., Smith, M. J., Beyreuther, K., Bush, A. I., and Masters, C. L. (1999) *Ann. Neurol.* **46,** 860–866
8. Lue, L. F., Kuo, Y. M., Roher, A. E., Brachova, L., Shen, Y., Sue, L., Beach, T., Kurth, J. H., Rydel, R. E., and Rogers, J. (1999) *Am. J. Pathol.* **155,** 853–862
9. Haass, C., and Selkoe, D. J. (2007) *Nat. Rev. Mol. Cell Biol.* **8,** 101–112
10. Baglioni, S., Casamenti, F., Bucciantini, M., Luheshi, L. M., Taddei, N., Chiti, F., Dobson, C. M., and Stefani, M. (2006) *J. Neurosci.* **26,** 8160–8167
11. Ross, C. A., and Poirier, M. A. (2005) *Nat. Rev. Mol. Cell Biol.* **6,** 891–898
12. Caughey, B., and Lansbury, P. T. (2003) *Annu. Rev. Neurosci.* **26,** 267–298
13. Glabe, C. G. (2006) *Neurobiol. Aging* **27,** 570–575
14. Hafner, J. H., Cheung, C. L., Woolley, A. T., and Lieber, C. M. (2001) *Prog. Biophys. Mol. Biol.* **77,** 73–110
15. Ding, T. T., Lee, S. J., Rochet, J. C., and Lansbury, P. T., Jr. (2002) *Biochemistry* **41,** 10209–10217
16. Lashuel, H. A., Hartley, D., Petre, B. M., Walz, T., and Lansbury, P. T., Jr. (2002) *Nature* **418,** 291
17. Lashuel, H. A., and Lansbury, P. T., Jr. (2006) *Q. Rev. Biophys.* **39,** 167–201
18. Kayed, R., Pensalfini, A., Margol, L., Sokolov, Y., Sarsoza, F., Head, E., Hall, J., and Glabe, C. (2009) *J. Biol. Chem.* **284,** 4230–4237
19. Montoya, M., and Gouaux, E. (2003) *Biochim. Biophys. Acta* **1609,** 19–27

20. Parker, M. W., and Feil, S. C. (2005) *Prog. Biophys. Mol. Biol.* **88,** 91–142
21. Glabe, C. G., and Kayed, R. (2006) *Neurology* **66,** S74–78
22. Burdick, D., Soreghan, B., Kwon, M., Kosmoski, J., Knauer, M., Henschen, A., Yates, J., Cotman, C., and Glabe, C. (1992) *J. Biol. Chem.* **267,** 546–554
23. Kayed, R., and Glabe, C. G. (2006) *Methods Enzymol.* **413,** 326–344
24. Kayed, R., Head, E., Sarsoza, F., Saing, T., Cotman, C. W., Necula, M., Margol, L., Wu, J., Breydo, L., Thompson, J. L., Rasool, S., Gurlo, T., Butler, P., and Glabe, C. G. (2007) *Mol. Neurodegener.* **2,** 18
25. Kayed, R., Head, E., Thompson, J. L., McIntire, T. M., Milton, S. C., Cotman, C. W., and Glabe, C. G. (2003) *Science* **300,** 486–489
26. Li, Q., Lau, A., Morris, T. J., Guo, L., Fordyce, C. B., and Stanley, E. F. (2004) *J. Neurosci.* **24,** 4070–4081
27. Kokubo, H., Kayed, R., Glabe, C. G., Staufenbiel, M., Saido, T. C., Iwata, N., and Yamaguchi, H. (2009) *Int. J. Alzheimers Dis.* **2009,** pii 689285
28. Shafrir, Y., Durell, S., Arispe, N., and Guy, H. R. (2010) *Proteins* **78,** 3473–3487
29. Yamamoto, N., Fukata, Y., Fukata, M., and Yanagisawa, K. (2007) *Biochim. Biophys. Acta* **1768,** 1128–1137
30. Zhu, M., Li, J., and Fink, A. L. (2003) *J. Biol. Chem.* **278,** 40186–40197
31. Chen, F. Y., Lee, M. T., and Huang, H. W. (2003) *Biophys. J.* **84,** 3751–3758
32. Modler, A. J., Gast, K., Lutsch, G., and Damaschun, G. (2003) *J. Mol. Biol.* **325,** 135–148
33. Porat, Y., Kolusheva, S., Jelinek, R., and Gazit, E. (2003) *Biochemistry* **42,** 10971–10977
34. Pountney, D. L., Lowe, R., Quilty, M., Vickers, J. C., Voelcker, N. H., and Gai, W. P. (2004) *Journal of Neurochemistry* **90,** 502–512
35. Arispe, N., Pollard, H. B., and Rojas, E. (1993) *Proc. Natl. Acad. Sci. U.S.A.* **90,** 10573–10577
36. Kagan, B. L., Hirakura, Y., Azimov, R., Azimova, R., and Lin, M. C. (2002) *Peptides* **23,** 1311–1315
37. Jang, H., Arce, F. T., Ramachandran, S., Capone, R., Azimova, R., Kagan, B. L., Nussinov, R., and Lal, R. (2010) *Proc. Natl. Acad. Sci. U.S.A.* **107,** 6538–6543
38. Yamaguchi, H., Maat-Schieman, M. L., van Duinen, S. G., Prins, F. A., Neeskens, P., Natté, R., and Roos, R. A. (2000) *J. Neuropathol. Exp. Neurol.* **59,** 723–732
39. Braak, H., and Braak, E. (1991) *Acta Neuropathol.* **82,** 239–259
40. Folstein, M. F., Folstein, S. E., and McHugh, P. R. (1975) *J. Psychiatr. Res.* **12,** 189–198